

# $\epsilon$ -Caprolactone/ $\text{ZnCl}_2$ Complex Formation: Characterization and Ring-Opening Polymerization Mechanism

GUSTAVO A. ABRAHAM,<sup>1,2</sup> ALBERTO GALLARDO,<sup>2</sup> ANGEL E. LOZANO,<sup>2</sup> JULIO SAN ROMAN<sup>2</sup>

<sup>1</sup> Instituto de Ciencia y Tecnología de Materiales (INTEMA), UNMDP-CONICET, Av. J.B. Justo 4302, 7600, Mar del Plata, Argentina

<sup>2</sup> Instituto de Ciencia y Tecnología de Polímeros, CSIC, Juan de la Cierva 3, 28006, Madrid, España

Received 8 November 1999; accepted 26 January 2000

**ABSTRACT:**  $\epsilon$ -Caprolactone ( $\epsilon$ -CL) has been mixed with  $\text{ZnCl}_2$  at different mol ratios. The resulting complex was characterized through  $^1\text{H}$  and  $^{13}\text{C}$  NMR spectroscopy in bulk and in solutions, differential scanning calorimetry (DSC), wide-angle X-ray diffraction (WAXD), and optical microscopy. Ring-opening polymerization of  $\epsilon$ -caprolactone [M] using  $\text{ZnCl}_2$  as an initiator [I] at different monomer/initiator ratios has been successfully performed in xylene. The molecular weight of poly( $\epsilon$ -caprolactone) (PCL) as measured by gel permeation chromatography (GPC) was found to depend linearly on the [M]/[I] ratio. Theoretical calculations were carried out to understand the geometry of the complex and the operating ring-opening mechanism. Both experimental and computational results and the presence of methylene–chloride end group, confirmed by NMR, are in agreement with a coordination–insertion mechanism for the ring-opening polymerization proposed in this article. © 2000 John Wiley & Sons, Inc. *J Polym Sci A: Polym Chem* 38: 1355–1365, 2000

**Keywords:** ring-opening polymerization; lactones; zinc chloride; mechanism, quantum-mechanical calculation

## INTRODUCTION

It is very well known that ring-opening polymerization (ROP) of lactones and related compounds is a very effective method for the synthesis of high molecular weight aliphatic polyesters.<sup>1,2</sup> ROP of lactones can be more or less efficiently initiated by several mechanisms, existing in a number of very effective initiators including metal halides, oxides, carboxylates, and alkoxides.<sup>1–5</sup> In this way, some organometallic compounds such as alkylmetals have been also used in polyester synthesis.

The polymerization of  $\epsilon$ -CL can be brought about by living polymerization, using various ini-

tiators such as bimetallic  $\mu$ -oxoalkoxides,<sup>6</sup> or aluminum porphyrin in the presence of alcohol.<sup>7</sup> In the last case, the growing species of the polymerization of  $\epsilon$ -CL is a (porphinato)aluminum alkoxide, formed by the insertion of  $\epsilon$ -CL into the Al–Cl bond of the initiator. Anionic polymerization of  $\epsilon$ -CL has been reported with potassium or lithium *tert*-butoxide, leading to a living ring-chain equilibrium system where cyclic oligomers are produced by back-biting degradation from the initially formed linear polymers.<sup>8</sup> Cationic polymerization of lactones by means of alkylsulfonates as well as various classes of cationic initiators were also investigated, and the mechanism has become a matter of controversy.<sup>9</sup>

Although halogenides of metals, such as  $\text{BF}_3$ ,  $\text{AlCl}_3$ ,  $\text{ZnCl}_2$ , and  $\text{SnCl}_4$  are strong Lewis acids and good catalysts to initiate the cationic polymerization of lactones, it has been reported that

Correspondence to: G. A. Abraham (E-mail: icta308@ictp.csic.es)

*Journal of Polymer Science: Part A: Polymer Chemistry*, Vol. 38, 1355–1365 (2000)  
© 2000 John Wiley & Sons, Inc.

some of these compounds can promote a coordination–insertion mechanism instead of a true cationic chain growth.<sup>10,11</sup> Because of the interest in biodegradable polymers with low toxicity, we have selected zinc chloride as a convenient initiator because of the presence of zinc in biological pathways and its lack of toxicity. In the case of lactone polymerization, zinc chloride has been suggested as a coordination initiator and not as a cationic (or acidic) one, and at the current state, only hypothetical schemes have been proposed from a mechanistical point of view.<sup>10–12</sup>

In this work we present a study of the interaction of a Lewis acid,  $\text{ZnCl}_2$ , and  $\epsilon$ -caprolactone describing the formation of a crystalline species ascribed to the stoichiometric complex  $\epsilon\text{-CL}/\text{ZnCl}_2$  (1 : 1). Moreover, computational and experimental evidences of the coordination–insertion mechanism proposed for the ring-opening polymerization are shown. The effect of the monomer/initiator ratio on the control of molecular weight of polymerized samples is also discussed.

## EXPERIMENTAL

### Monomer–Initiator Mixtures Preparation and Polymerization

$\epsilon$ -Caprolactone (Merck-Schuchardt) was dried and distilled under vacuum, zinc chloride (Probus) was dried under vacuum during 24 h, and xylene for synthesis (Panreac Química S.A., Spain) was used as received.

To study the complex formation, mixtures of  $\epsilon$ -caprolactone and  $\text{ZnCl}_2$  were prepared at different mol ratios (0.5 : 1, 1 : 1, 2 : 1, and 3 : 1). A slight heating and stirring was applied to make easier the solubility of the inorganic salt in the monomer. Ring-opening polymerization of  $\epsilon$ -caprolactone was performed in xylene solution. Different  $[\text{M}]/[\text{I}]$  ratio mixtures were polymerized (i.e., 2 : 1; 5 : 1; 10 : 1, and 30 : 1). Anhydrous  $\text{ZnCl}_2$  was first dissolved in 80 mL of xylene under stirring, and 5 mL  $\epsilon$ -caprolactone (47 mmol) was then added. The reaction was carried out in a 250-mL two-neck flask using a coil condenser coupled to a Dean–Stark to separate water traces. The flask was immersed into a thermostated heating bath at the solvent boiling temperature (135 °C). Samples were collected from the master batch at appropriate times, and the polymer was isolated by pouring it into an excess of ethanol containing a small amount of hydrochloric acid to

remove the initiator residue in the polymer. Afterward, the polymer was filtered and exhaustive dried. The samples collected for GPC analysis were directly dried under high vacuum ( $10^{-3}$  mm Hg) during 24 h at room temperature.

### Characterization

Differential scanning calorimetry experiments were carried out in a Perkin–Elmer DSC-4. Two scans were performed by using a 5 °C/min heating rate and a 320 °C/min cooling rate (quenching) between runs. Thermograms were obtained in the range –50 to 70 °C under nitrogen purge.

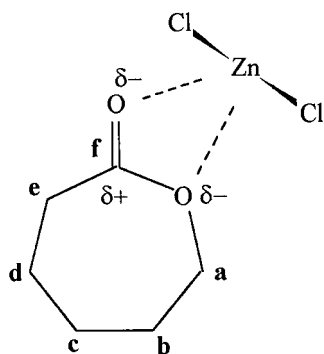
$^1\text{H}$  and  $^{13}\text{C}$  nuclear magnetic resonance spectra of the monomer/initiator mixtures were performed in a Varian XLR-300 NMR spectrometer operating at 75.5 MHz for  $^{13}\text{C}$  and 300 MHz for  $^1\text{H}$  measurements. NMR measurements of bulk samples were performed at 80 °C (melting point 60–65 °C). In this case, the measurements were conducted in 0.5 mm i.d. capillary tubes within 5 mm o.d. sample tubes containing  $\text{DMSO-d}_6$ . A delay time between pulses of 2 s for  $^{13}\text{C}$  measurements was applied. Samples for polymer characterization were measured in a Varian Gemini 200 MHz NMR spectrometer at room temperature. The 200-MHz  $^1\text{H}$  NMR spectra was obtained from 5% (w/v)  $\text{CDCl}_3$  solutions and the 50-MHz  $^{13}\text{C}$  NMR one from 25% (w/v)  $\text{CDCl}_3$  solutions.

Molecular weights and molecular weight distributions were determined by using a Perkin–Elmer gel permeation chromatograph equipped with a refractive index detector series 200. A set of  $10^4$ ,  $10^3$ , and 500 Å PL-gel columns conditioned at 25 °C were used to elute the samples of 10 mg/mL concentration at 1 mL/min HPLC-grade chloroform flow rate. Polystyrene standards were used for calibration.

Wide-angle X-ray diffraction (WAXD) patterns were obtained by means of a Philips X-ray diffractometer using  $\text{Cu K}_\alpha$  radiation. Optical micrographs of crystalline samples were taken in a Nikon Microscope, eclipse E400 model, using a dark field.

### Computational Methods

Initial geometries were obtained by AM1<sup>13</sup> quantum-mechanical semiempirical calculations by using the original parameters of this program, based on the restricted Hartree–Fock (RHF) method, included in MOPAC version 6.0.<sup>14</sup> The MOPAC program ran on a Silicon Graphics Indi-



**Scheme 1a.** Coordination between  $\epsilon$ -CL and  $\text{ZnCl}_2$ .

go2 R-10000 workstation using as graphics interface and data analysis the Cerius<sup>2</sup> program.<sup>15</sup> The AM1 semiempirical method is commonly accepted to allow a better description of the lone-pair/lone-pair repulsion in several compounds.<sup>16</sup> The geometrical optimizations results were used as input data for the semiempirical calculations. Geometries were optimized as internal coordinates. The optimization was stopped when Herbert or Peter tests were satisfied in the Broyden-Fletcher-Goldfarb-Shanno (BFGS) method.<sup>17</sup> *Ab initio*<sup>18</sup> calculations were made with the Gaussian 98 package<sup>19</sup> using as data and graphical interface the Cerius<sup>2</sup> program.<sup>15</sup> Through the Z-matrix input data from a semiempirical AM1 calculation, the geometry and the total electronic energy were calculated by the RHF method with 6-31G(d) (RHF/6-31G\*) basis set.

The PRECISE keyword was applied for semiempirical calculations during the optimization process, with the gradient norm set to 0.01, whereas the FOPT keyword was used for all *ab initio* calculations. These semiempirical and *ab initio* calculations were carried out with full geometry optimization (bond lengths, bond angles, and dihedral angles) without any assumption of symmetry for both methodologies.

Mulliken population analyses<sup>20</sup> used to discuss the electronic distributions (charges) are adequate for present purposes because they reflect the trends in populations and charges that seem to be important rather than their actual values.

## RESULTS AND DISCUSSION

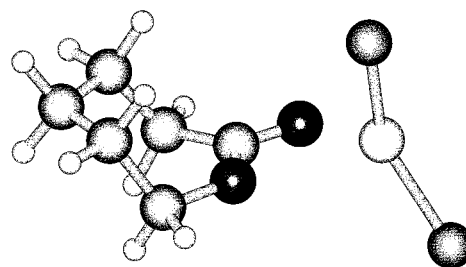
### $\epsilon$ -CL/ $\text{ZnCl}_2$ Complex Formation and Characterization

Although Zn halogenides have been classically considered as Lewis acid agents in the ROP of

lactones via cationic polymerization, several works have reported that  $\text{ZnCl}_2$  and other metal halogenides initiate the ring-opening polymerization by a coordination-insertion mechanism.<sup>7,21</sup> The stoichiometric interaction between Zn and both exocyclic and endocyclic oxygen atoms of the lactone (Scheme 1a) has been suggested as a tentative coordination mechanism for Zn halogenides. To understand the interactions between both components, and consequently, the ROP polymerization mechanism of this  $\epsilon$ -lactone, we have studied the behavior of different mixtures  $\epsilon$ -caprolactone/ $\text{ZnCl}_2$ .

Decoupled <sup>13</sup>C NMR spectroscopy for a series of mixtures was performed to analyze the chemical shift of the carbon atoms that seems to be directly involved in the coordination step. Mixtures prepared with different  $\epsilon$ -CL/ $\text{ZnCl}_2$  mol ratio (i.e., 1 : 1, 2 : 1, and 3 : 1) gave us a first evidence of the mentioned interaction. The plot of the NMR signal values of carbonyl carbons Cf and Ca (which are the carbons bound to the oxygen atoms) as a function of the [M]/[I] ratio, showed an inverse linear relationship. This result is in agreement with a strong interaction between the metal and both oxygen atoms [Fig. 1(a) and (b)]. Thus, the shifting of the signals can be related to the formation of complexes  $\epsilon$ -CL/ $\text{ZnCl}_2$ . The spectra of samples containing excess of  $\text{ZnCl}_2$  could not be obtained due to the solid nature of the adduct.

Moreover, chloroform solutions of different [M]/[I] mol ratio samples (including a sample with an excess of  $\text{ZnCl}_2$ ) exhibited the same downfield shift of the <sup>13</sup>C NMR resonance of the carbons Cf and Ca than the bulk samples. However, in this case, the variation is less pronounced. These differences with respect to the bulk solutions could be ascribed to the solvent influence in the dissociation equilibrium of the molecular complex. This agrees with the results obtained when DMSO-*d*<sub>6</sub> was used instead of chloroform as sol-

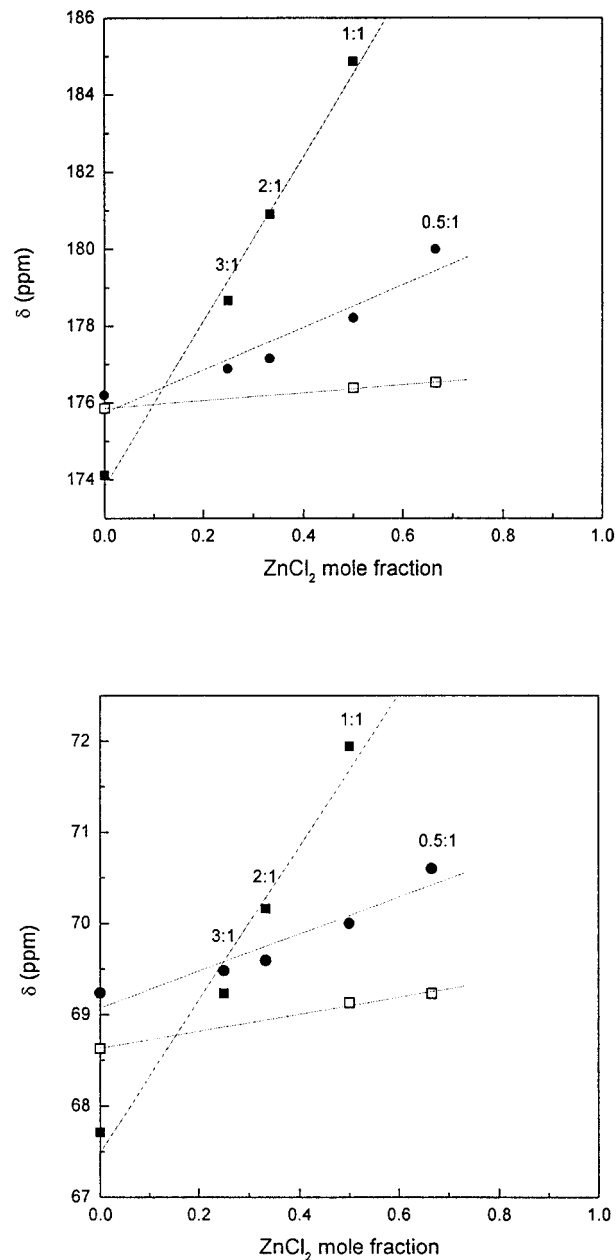


**Scheme 1b.** Optimized structure of the complex  $\epsilon$ -CL/ $\text{ZnCl}_2$ .

vent. In this case, the carbonyl carbon signal exhibited a chemical shift independent of the  $\text{ZnCl}_2$  concentration. As  $\text{DMSO-d}_6$  is a strong polar solvent, with a high solvating capability, the polar interactions of the solvent with the lactone group are favored instead of the lactone- $\text{ZnCl}_2$  ones.

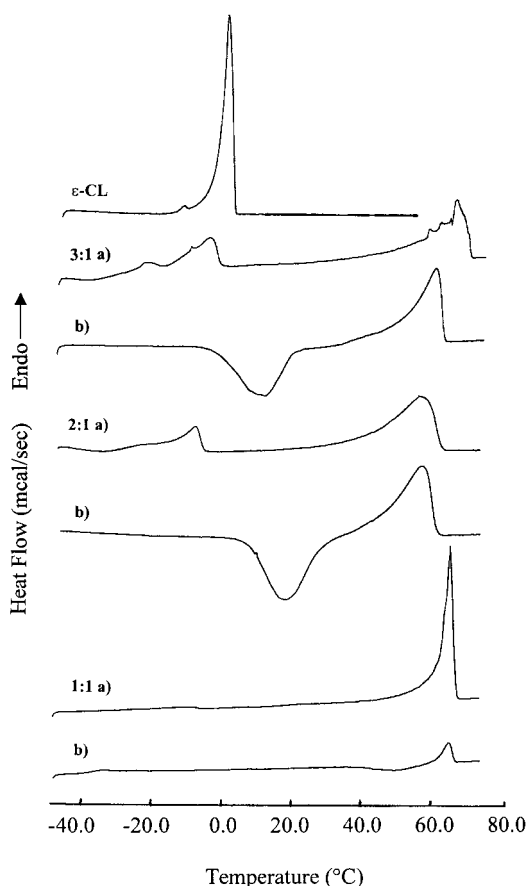
On the other hand,  $\epsilon\text{-CL}/\text{ZnCl}_2$  mixtures handling leads to the formation of a true, stable crystalline species. Crystallization was produced 2 weeks after solution preparation at room temperature. DSC analysis of these samples shows a correlative decrease of both, the  $\epsilon\text{-caprolactone}$  melting point and the melting enthalpy, with the concentration (pure  $\epsilon\text{-CL}$  exhibited a melting point at  $-0.6^\circ\text{C}$ ) as well as the appearance of a new endothermic peak, which has been assigned to the melting of a complex  $\epsilon\text{-caprolactone}/\text{ZnCl}_2$ . The thermogram of the stoichiometric complex (1 : 1) (Fig. 2) corresponding to the first scan of the slowly crystallized complex present a sharp endothermic melting point at  $65.6^\circ\text{C}$ . In a second run after quenching from melt, the recrystallization seems to be somewhat hindered, but a small endothermic peak appears at the same temperature. Probably, this is a result of the high viscosity of the melt system that hinders the tridimensional reorganization of the complexed species. For non-stoichiometric solutions, the thermograms displayed in the same figure are more clear. In the case of the 2 : 1 mol ratio complex, there is an excess of  $\epsilon\text{-CL}$ , which is clearly associated with the exothermic peak at  $-7.7^\circ\text{C}$  of noncomplexed  $\epsilon\text{-CL}$ , which in addition, acts as a partial diluent of the crystallized  $\epsilon\text{-CL}/\text{ZnCl}_2$  complex, giving rise to the broadening of the melt transition and the depression of the melting point. However, after quenching, the viscosity of the solution is lower and a recrystallization and the subsequent melting peaks are well observed in the second scan. The same behavior is observed for the more diluted system corresponding to a 3 : 1 mol ratio. It is important to stress that in the case of the stoichiometric system, the melting peak associated to free  $\epsilon\text{-CL}$  was not observed, suggesting that virtually all  $\epsilon\text{-caprolactone}$  is complexed with zinc chloride. According to this, the complex is assigned to a stoichiometric ratio  $\epsilon\text{-CL}/\text{ZnCl}_2$ .

Figure 3 shows WAXD patterns of  $\text{ZnCl}_2$  and the  $\epsilon\text{-CL}/\text{ZnCl}_2$  complex (1 : 1 and 3 : 1 mol ratio).  $\text{ZnCl}_2$  exhibited its typical pattern of sharp crystalline peaks, having a tetrahedral geometry. It is observed that the complex 1 : 1 has two broad crystalline peaks—one at  $2\theta = 21.63^\circ$  (with a shoulder at  $22.3^\circ$ ), and the other at  $2\theta = 24^\circ$ . On



**Figure 1.**  $^{13}\text{C}$  NMR chemical shift as a function of the  $\text{ZnCl}_2$  concentration. (a) Carbonyl carbon (carbon Cf); (b) carbon Ca. (■) bulk samples at  $80^\circ\text{C}$ . (●)  $\text{CDCl}_3$  solution at  $20^\circ\text{C}$ . (□)  $\text{DMSO-d}_6$  solution at  $20^\circ\text{C}$ .

the other hand, the complex 3 : 1 also has two peaks at  $2\theta = 21.2^\circ$  and  $23.56^\circ$ , respectively. The few peaks present in these patterns give evidence of the existence of a single phase with a high symmetry. In both patterns there were no peaks related to  $\text{ZnCl}_2$ , confirming its total complexation with  $\epsilon\text{-CL}$ . Moreover, the observation of an amorphous band in the  $\epsilon\text{-CL}/\text{ZnCl}_2$  complex 3 : 1



**Figure 2.** DSC thermograms of  $\epsilon$ -CL and different  $\epsilon$ -CL/ZnCl<sub>2</sub> mixtures. (a) First scan; (b) second scan.

could be ascribed to the presence of noncomplexed  $\epsilon$ -CL, as was discussed above.

Figure 4(a) and (b) shows the morphology of these systems. The stoichiometric complex forms relatively small lamellar crystals when the system is allowed to stay without agitation during 1 or 2 weeks at room temperature. The lamellar structure of the crystals is better observed for the system with  $\epsilon$ -CL/ZnCl<sub>2</sub> 3 : 1 mol ratio. In this case, the excess of  $\epsilon$ -CL acts as a diluent, and allows the growth of the lamellar morphology to give relatively big crystals that are well observed by optical microscopy under a dark field.

#### Theoretical Calculations and Polymerization Mechanism

To figure out the mechanism pathway of the polymerization, a theoretical study has been carried out. According to Scheme 1, the complex  $\epsilon$ -CL/ZnCl<sub>2</sub> and complexes of different Lewis acids such

as [ZnCl]<sup>+</sup>, [Zn-Acetate]<sup>+</sup>, Li<sup>+</sup>, and LiCl were calculated by *ab initio* methods using the HF/6-31G\* basis set. The geometrical parameters of the  $\epsilon$ -CL/ZnCl<sub>2</sub> complex showed that zinc coordination occurs in both lactone oxygens, in contrast to those results found for the complex [ $\epsilon$ -CL/Li]<sup>+</sup> and  $\epsilon$ -CL/LiCl. In this way, whereas a 1 : 1 complex between lithium chloride and the exocyclic oxygen is typical for Lewis acids with free *p*-orbitals, a more complex interaction exists with Zn compounds. Although Zn forms no compound in which the *d* shell is other than full, there is some resemblance to the *d*-group elements in their ability to form complexes.<sup>22</sup>

The interatomic distances of some bonds of interest in respect to noncomplexed  $\epsilon$ -CL are shown in Table I. Regarding the geometric and electronic results given in Table I, several points can be outlined. First, the alkyl-oxygen (Ca—O) bond distance increases in comparison with the noncomplexed  $\epsilon$ -CL, while the acyl-oxygen (Cf—O) bond distance decreases. Second, an electronic deficiency increase was observed in the carbon Ca for the complex while the LUMO energy decreases. This fact determines Ca to be susceptible to a nucleophilic attack. Furthermore, the computational results revealed that Zn is placed in a slight asymmetric position respect to the lactone group, being a chlorine atom bond distance larger

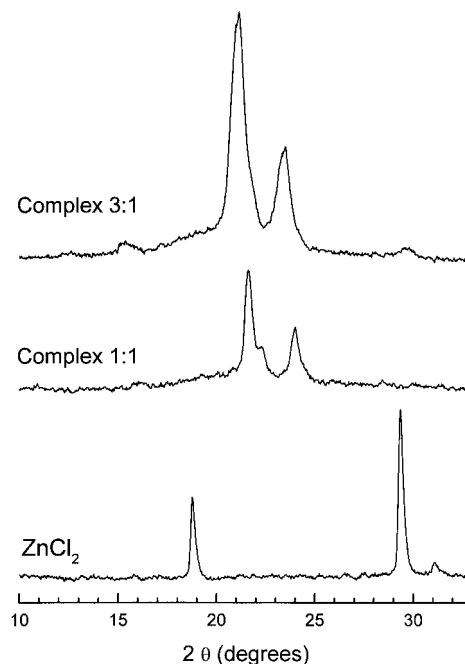


**Figure 3.** WAXD patterns: ZnCl<sub>2</sub>; and  $\epsilon$ -CL/ZnCl<sub>2</sub> complex: 1 : 1 mol ratio; 3 : 1 mol ratio.

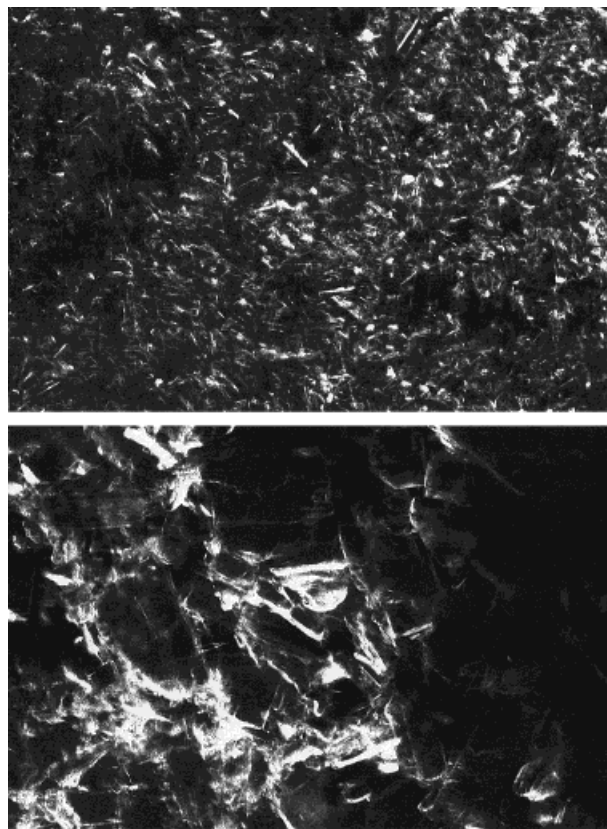


**Figure 4.** Optical micrographs (10.6 $\times$ ) of crystallized  $\epsilon$ -CL/ $\text{ZnCl}_2$  complex: (a) 2 : 1 mol ratio; (b) 3 : 1 mol ratio.

than the other one. When small variations in the Zn—Cl bond distance are introduced, two important facts are observed: a change in the alkyl-oxygen distance, and a significant variation in both the electronic density and the LUMO energy. Thus, when the bond distance of a chlorine atom is enlarged, an increase in the carbon **Ca** reactivity towards nucleophiles appears. The HOMO and LUMO energies as well as the electronic density of carbon **Ca** are given in Table II.

Moreover, the modelization displacing a chlorine atom far away from the metallic center (bond distance higher than 4 Å) brought about a stretching of 3.95% in the alkyl-oxygen bond distance, indicating that the cationic species  $[\text{ZnCl}]^+$  extraordinarily activates carbon **Ca** of  $\epsilon$ -CL for a nucleophilic reaction.

These geometrical and electronic results gave us an idea of the possible mechanism operating for the ring-opening polymerization. Consequently, we have proposed a new scheme for the polymerization of  $\epsilon$ -CL with  $\text{ZnCl}_2$  as the initiator; this new coordination–insertion mechanism is shown in Scheme 2, and it is in very good agreement with the experimental evidences and theoretical calculations. After the initial coordination (Scheme 1b), already described above, a chlorine atom is transferred to carbon **Ca** leading to a  $\omega$ -chloro carboxylate coordinated with  $[\text{ZnR}]^+$ , where R is a chlorine atom, or another  $\omega$ -chloro carboxylate if the second chlorine is removed.

**Table I.** Variation of the Internuclear Distances of  $\epsilon$ -CL with Different Species Respect to Noncomplexed  $\epsilon$ -CL

Bond	Distance of Reference ( $\text{\AA}$ ) $\epsilon$ -CL	Distance Variation Calculated with <i>ab initio</i> Method (%)				
		$\text{ZnCl}_2$	$[\text{ZnCl}]^+$	$[\text{Zn-Acetate}]^+$	$\text{Li}^+$	$\text{LiCl}$
Ce—Cf	1.515	−0.97	−1.28	−1.14	−0.78	−0.53
Cf=O	1.185	2.05	4.64	4.69	3.04	1.70
Cf—O	1.333	−2.05	−3.89	−3.64	−3.18	−2.02
O—Ca	1.416	1.63	3.95	3.53	2.36	1.12
Ca—Cb	1.523	−0.21	−0.41	−0.23	−0.29	−0.14

Bond	Distance of Reference ( $\text{\AA}$ ) $\epsilon$ -CL	Distance Variation Calculated with AM1 Method (%)				
		$\text{ZnCl}_2$	$[\text{ZnCl}]^+$	$[\text{Zn-Acetate}]^+$	$\text{BF}_3$	$[\text{CH}_3\text{O}]^-$
Ce—Cf	1.497	0.01	−0.18	−0.15	−0.09	3.87
Cf=O	1.232	0.75	3.56	0.20	1.33	4.25
Cf—O	1.373	−0.71	−2.53	−2.60	−1.22	6.28
O—Ca	1.426	0.40	2.16	1.93	0.50	−1.83
Ca—Cb	1.517	−0.09	−0.45	−0.40	−0.06	0.64

**Table II.** Molecular Orbital Energies Estimated by *ab initio* Calculations

Species	$E_{\text{HOMO}}$ (eV)	$E_{\text{LUMO}}$ (eV)	$E_{\text{GAP}}^{\text{a}}$ (eV)	Carbon <b>a</b> Charge <sup>b</sup>
$\epsilon$ -CL	-11.54	5.20	-16.74	0.351
$\epsilon$ -CL/LiCl	-9.13	2.40	-11.53	0.384
$\epsilon$ -CL/ZnCl <sub>2</sub>	-10.83	2.98	-13.81	0.398
[ $\epsilon$ -CL/Li] <sup>+</sup>	-16.04	-3.22	-12.82	0.398
[ $\epsilon$ -CL/ZnCl] <sup>+</sup>	-15.61	-2.51	-13.10	0.429
[ $\epsilon$ -CL/Zn/Acetate] <sup>+</sup>	-16.03	-1.52	-14.51	0.419

<sup>a</sup> Energy gap,  $E_{\text{GAP}} = E_{\text{HOMO}} - E_{\text{LUMO}}$ <sup>b</sup> Atomic charge with hydrogens summed into carbon atom.

Therefore, we suggest that there is a competition between the monomer (cyclic form) and the  $\omega$ -chloro carboxylate for the Zn coordination in the neutral species **A**. This species is in equilibrium with species **B**, which has a positive global charge. It is possible that the chlorine group in **B** is displaced by a carboxylate group, and the primary species has a tetracoordinated Zn atom. In any case, the positive global charge and the low LUMO energy along with the high LUMO coefficient on the carbon **Ca** determine a high activation of that atom toward the attack of a nucleophilic species like a  $\omega$ -chloro carboxylate. These later steps define a propagation stage, and propose that the existence of cationic species like that are directly responsible of the activation of the carbon **Ca** in lactones with a subsequent insertion of new monomeric units leading to polymerization by the mechanism described above.

In conclusion, it has been estimated that the species **B** has an increase of 3.53% in the alkyl-oxygen bond distance in comparison with  $\epsilon$ -CL, showing an interesting conformational structure. Thus, if **R** has a carboxylate group, this group tends to adopt a perpendicular position in respect to the lactone plane. This structure has been calculated for the case of an acetate group, and the optimized geometry is shown in Scheme 3. The Zn atom present in **B** is tetracoordinated, being the Lewis acid a [Zn-Acetate]<sup>+</sup> moiety.

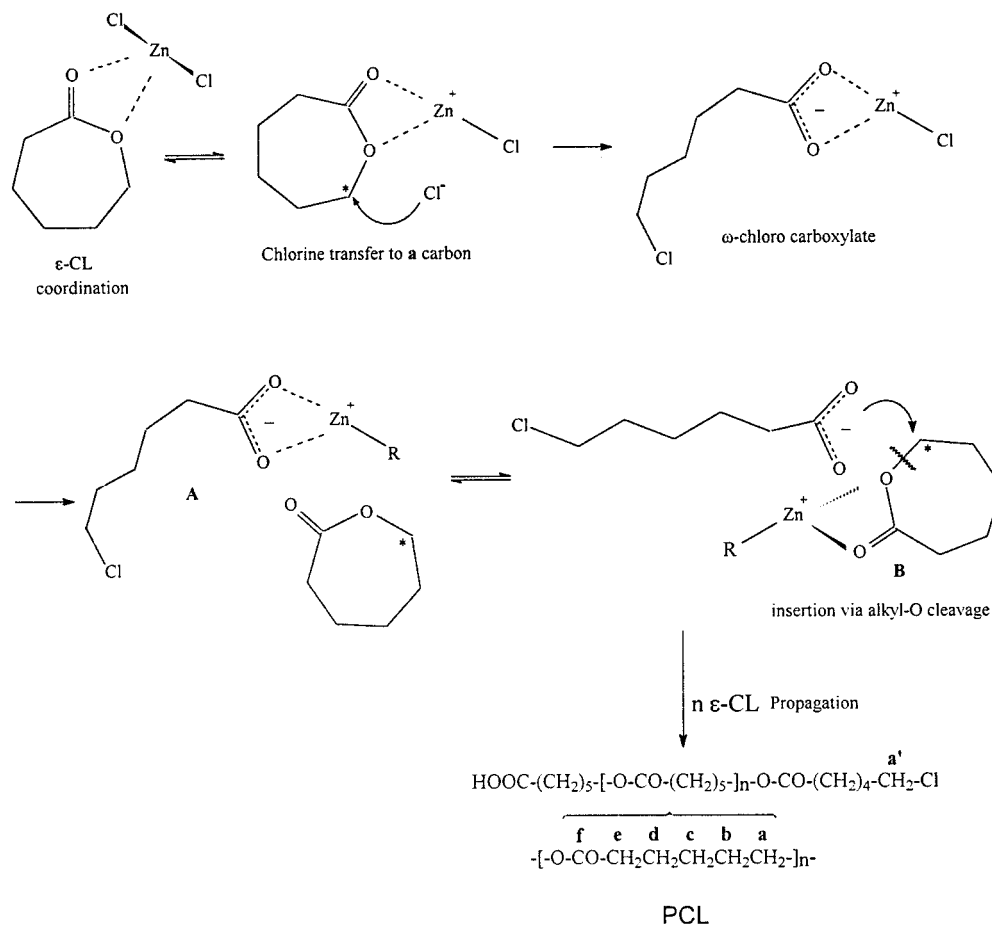
The same calculations have been repeated by using the AM1 semiempirical method. The results showed a similar trend for both molecules and complexes, as it is also presented in Table I. This less CPU-intensive quantum-mechanical method would allow to modelize much larger structures or incorporate other features as tacticity. Thus, the interaction of  $\epsilon$ -caprolactone with a methoxy group

has been evaluated to predict the behavior of metal alkoxides in ROP processes. In this case, an opposite effect was observed. The reaction model showed that the alkyl-oxygen bond distance decreased, whereas the acyl-oxygen bond distance increased. Therefore, as it should be expected with this type of initiator, the ring-opening polymerization proceeds via acyl-oxygen bond cleavage.<sup>23</sup>

### Polymerization

The results obtained from the complex studies and the computational analysis suggest that ZnCl<sub>2</sub> could initiate the ROP of  $\epsilon$ -caprolactone by means of the proposed coordination–insertion mechanism.

In this way, a series of polymerization reactions were performed using different [M]/[I] ratios in reflux of xylene as it is described in the Experimental section. Samples were collected at different times and analyzed by <sup>1</sup>H NMR and GPC after exhaustive drying. The evolution of the apparent molecular weight ( $M_w$ , weight-average) vs the reaction time is represented in Figure 5. As it was to be expected,  $\epsilon$ -caprolactone homopolymerizes well in the presence of ZnCl<sub>2</sub>, and the [M]/[I] ratio defines the limiting  $M_w$ . A decreasing of [M]/[I] ratio results in a lower average chain length, which means that the initiator takes part of the active chain end. This result is in agreement with the proposed coordination–insertion mechanism. The limiting  $M_w$  is plotted vs the [M]/[I] ratio in Figure 6, giving a good linear relationship that indicates the reliability and reproducibility of the reaction. Thus, it is possible to control the molecular weight of the polycaprolactone by this polymerization method in a wide

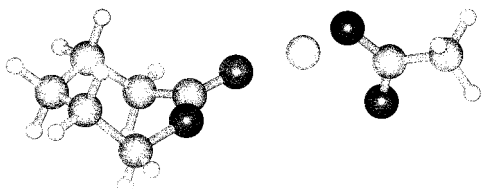


where R = Cl or  $\omega$ -chloro carboxylate if the second Cl is removed

**Scheme 2.** Coordination–insertion mechanism proposed to ring-opening polymerization.

interval of molecular weight values, including high molecular weights.

The conversion degree, calculated from NMR measurements, is shown in Figure 7(a) for  $[M]/[I] = 5 : 1$ , while both weight-average and number-



**Scheme 3.** Structure of complex **B** showing the tetra-coordination of Zn with a lactone and an acetate group.

average molecular weights as a function of conversion are displayed in Figure 7(b) for the same mol ratio. The  $M_w$  values as well as the  $M_n$  values were proportional to the conversion until a conversion of 0.65 was achieved. After reaching this point, a decreasing in the  $M_n$  values occurs, and a subsequent broadening of the polydispersity values from 1.9 to 2.5 is produced with the advance of the reaction. This result is probably associated to degradation or back-biting reactions inherent to processes at high temperatures and long times, which are well described for this kind of polymerization process. The low efficiency of the initiator is evidenced by the fact that the  $M_w$  apparent values are higher than those expected from the feed  $[M]/[I]$  ratio.



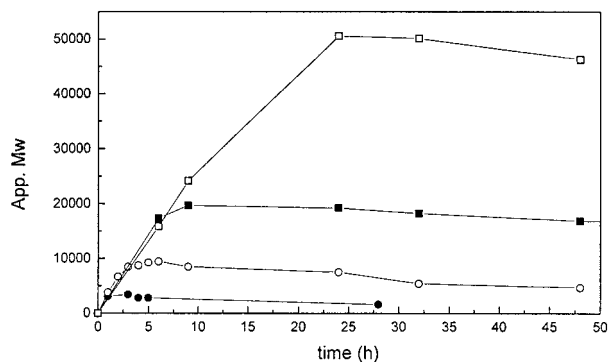


**Figure 5.** Apparent  $M_w$  evolution as a function of polymerization time for different  $[\text{M}]/[\text{I}]$  ratios. (●) 2 : 1; (○) 5 : 1; (■) 10 : 1; (□) 30 : 1.

The successful elucidation of the polymerization mechanism requires unambiguous identification of end groups. The  $^1\text{H}$  NMR analysis of the obtained polymers gave us another evidence of the proposed coordination–insertion mechanism. The observation of a triplet at 3.5 ppm was ascribed to a methylene end group capped with a chloride atom. Assignment of this triplet to the possible  $\text{CH}_2\text{—OH}$  end group has to be discarded because the derivatization with trifluoroacetic anhydride (TFA) did not shift this signal, as seen in Figure 8(a). The same method has been reported for the case of  $\text{ZnBr}_2$ -initiated polymerization of  $\epsilon\text{-CL}$ <sup>11</sup> and  $\text{SnBr}_4$ -initiated polymerization of L-lactide.<sup>24</sup> We have synthesized OH-ended PCL in the absence of catalysts by a polycondensation reaction as proposed by Fukuzaki.<sup>25</sup> In Figure 8(b) is shown the shifting of the characteristic signal of the methylene group adjacent to the hydroxyl functionality. This effect was obviously

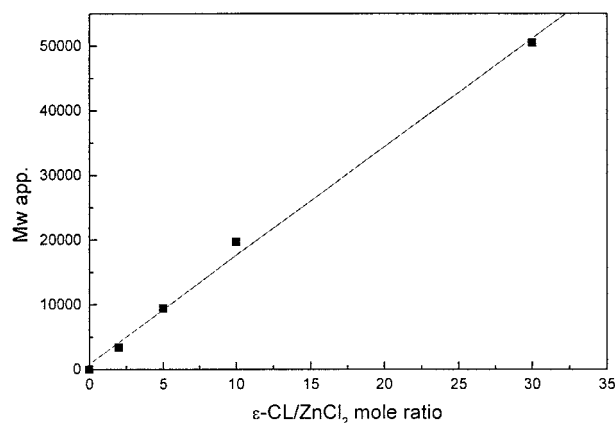


**Figure 6.** Apparent  $M_w$  at limit conversion as a function of the  $[\text{M}]/[\text{I}]$  mol ratio.

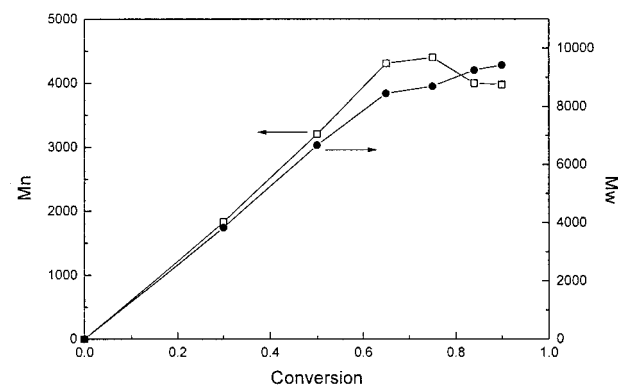
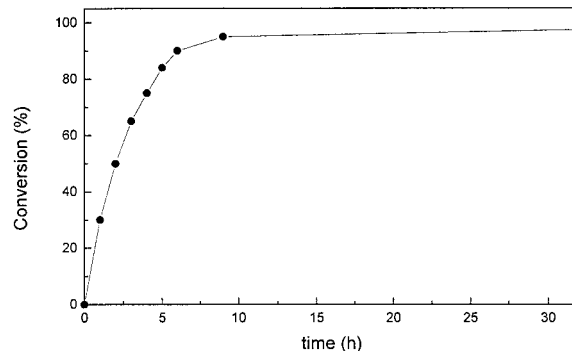


**Figure 7.** (a) Conversion as a function of polymerization time for  $[\text{M}]/[\text{I}] = 5 : 1$ . (b) Number-average molecular weight ( $M_n$ ) and weight-average molecular weight ( $M_w$ ) as a function of the conversion for  $[\text{M}]/[\text{I}] = 5 : 1$ .

not observable for Cl end groups, as mentioned above. The presence of a  $\omega$ -carboxylic end groups was confirmed by  $^{13}\text{C}$  NMR. The signal at 178 ppm was assigned to the carbons of carboxylic acid end groups. This analysis could only be performed with samples at low mol ratios (i.e., 2 : 1) and low reaction times.<sup>26</sup> Finally, it has been reported that true cationic initiators, such as fluoro-sulfonic acid, boron trifluoride, or methyl fluoro-sulfate, cause rapid degradation at temperatures above 50 °C that limit both yield and molecular weight of the resulting polymers.<sup>9</sup> Due to the absence of degradation products at the temperature used in this work, a cationic polymerization mechanism using  $\text{ZnCl}_2$  is not feasible.

## CONCLUSIONS

$\text{ZnCl}_2$  forms stable stoichiometric complexes with  $\epsilon$ -caprolactone that activate the process of ring-

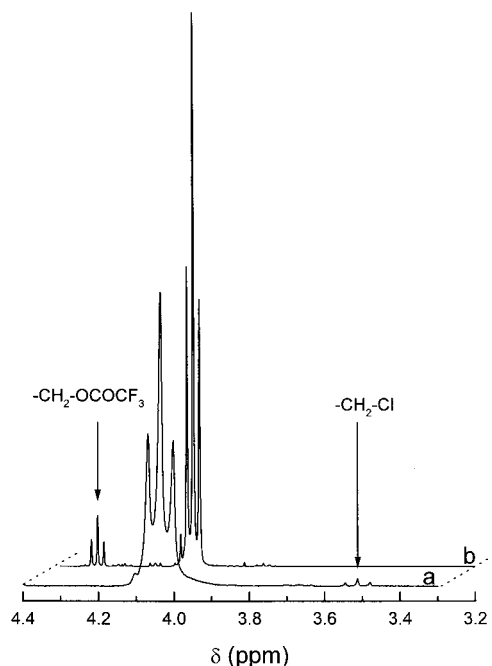


**Figure 8.**  $^1\text{H}$  NMR spectra: (a) PCL ( $[\text{M}]/[\text{I}] = 10 : 1$ , 24 h) after derivatization with TFA; (b) PCL synthesized without any catalyst after derivatization with TFA.

opening polymerization via an insertion–coordination mechanism. The complexation equilibrium is well visualized by  $^{13}\text{C}$  NMR spectroscopy, which makes clear the existence of an interaction of the carbonyl-oxy group of  $\epsilon$ -CL with zinc chloride. The resulting complex could be successfully characterized through NMR, DSC, WAXD, and optical microscopy.

The synthesized poly( $\epsilon$ -caprolactone) had a chlorine atom in the end of the chain, as was elucidated by NMR spectroscopy, confirming the transference of a chlorine atom in the first step of the mechanism. Both experimental and theoretical results suggest that the coordination–insertion mechanism seems to be the polymerization mechanism operating in this reaction.

Moreover, the molecular weight of PCL can be accurately controlled by the ratio  $\epsilon$ -CL/ $\text{ZnCl}_2$  being possible to achieve high molecular weight at temperatures up to 135 °C adjusting the  $[\text{M}]/[\text{I}]$  mol ratio.

G. Abraham thanks the Institute of Polymers Science and Technology, CSIC, Spain, as well as National Research Council of Argentina for the fellowship awarded. We also would like to thank Dr. Antonio Salinas for his

useful discussion about WAXD experiments and Comision Interministerial de Ciencia y Tecnología de España (MAT98-0964 and MAT98-0942).

## REFERENCES AND NOTES

- Löfgren, A.; Albertsson, A.-C.; Dubois, P.; Jérôme, R. *J. Mater Sci Rev Macromol Chem Phys* 1995, C35, 379–418.
- Johns, D. B.; Lenz, R. W.; Luecke, A. In *Ring-Opening Polymerization*; Ivin, K. J.; Saegusa, T., Eds.; Elsevier Applied Science: London, 1984; p. 461, vol. 1.
- Dubois, Ph.; Jérôme, R.; Teyssié, Ph. *Makromol Chem Macromol Symp* 1991, 42/43, 103.
- Dubois, Ph.; Ropson, N.; Jérôme, R.; Teyssié, Ph. *Macromolecules* 1996, 29, 1965.
- Schwach, G.; Coudane, J.; Engel, R.; Vert, M. *Polym Bull* 1994, 32, 617.
- Hamitou, A.; Ouhadi, T.; Jérôme, R.; Teyssié, P. *J Polym Sci Polym Chem Ed* 1977, 15, 865.
- Endo, M.; Aida, T.; Inoue, S. *Macromolecules* 1987, 20, 2982.
- Ito, K.; Hashizuka, Y.; Yamashita, Y. *Macromolecules* 1977, 10, 821.
- Jonté, J. M.; Dunsing, R.; Kricheldorf, H. R. *J Macromol Sci Chem* 1986, A23, 495.
- Kricheldorf, H. R.; Mang, T.; Jonte, J. M. *Macromolecules* 1984, 17, 2173.
- Kricheldorf, H. R.; Sumbél, M. *Makromol Chem* 1988, 189, 317.
- Kricheldorf, H. R.; personal communication.
- Shuman, D. A.; Robins, M. J.; Robins, R. K. *J Am Chem Soc* 1969, 91, 3391.
- MOPAC version 6.0. *Quant Chem Prog Exch* 1990, 445.
- Cerius<sup>2</sup> version 3.5. Biosym/Molecular Simulations Inc., 1995.
- Dewar, M. J. S.; Zoebish, E. G.; Healey, E. F.; Stewart, J. J. P. *J Am Chem Soc* 1985, 107, 3902.
- Anders, E.; Koch, R.; Freunsch, P. *J Comput Chem* 1993, 14, 1301.
- Hehre, W. T.; Radom, L.; Schleyer, P. von R.; Pople, J. A. In *Ab initio Molecular Orbital Theory*. John Wiley & Sons: New York, 1986.
- Frisch, M. J.; Trucks, G. W.; Schlegel, H. B.; Scuseria, G. E.; Robb, M. A.; Cheeseman, J. R.; Zakrzewski, V. G.; Montgomery, J. A., Jr.; Stratmann, R. E.; Burant, J. C.; Dapprich, S.; Millam, J. M.; Daniels, A. D.; Kudin, K. N.; Strain, M. C.; Farkas, O.; Tomasi, J.; Barone, V.; Cossi, M.; Cammi, R.; Mennucci, B.; Pomelli, C.; Adamo, C.; Clifford, S.; Ochterski, J.; Petersson, G. A.; Ayala, P. Y.; Cui, Q.; Morokuma, K.; Malick, D. K.; Rabuck, A. D.; Raghavachari, K.; Foresman, J. B.; Cioslowski, J.; Ortiz, J. V.; Stefanov, B. B.; Liu, G.; Liashenko, A.; Piskorz,

- P.; Komaromi, I.; Gomperts, R.; Martin, R. L.; Fox, D. J.; Keith, T.; Al-Laham, M. A.; Peng, C. Y.; Nanayakkara, A.; Gonzalez, C.; Challacombe, M.; Gill, P. M. W.; Johnson, B.; Chen, W.; Wong, M. W.; Andres, J. L.; Gonzalez, C.; Head-Gordon, M.; Replogle, E. S.; Pople, J. A. Gaussian 98, Revision A.3, 1998 Gaussian, Inc., Pittsburgh, PA.
20. Mulliken, R. S. *J Chem Phys* 1985, 23, 1833.
  21. Kricheldorf, H. R.; Mang, T.; Jonté, J. M. *Macromolecules* 1984, 17, 2173.
  22. Cotton, F. A.; Wilkinson, G. In *Advanced Inorganic Chemistry*; J. Wiley & Sons: New York, 1980.
  23. Dubois, Ph.; Jacobs, C.; Jérôme, R.; Teyssié, Ph. *Macromolecules* 1991, 24, 2266.
  24. Kricheldorf, H. R.; Sumbél, M. *Eur Polym J* 1989, 25, 585.
  25. Fukuzaki, H.; Yoshida, M.; Asano, M.; Aiba, Y. Kaetsu, I. *Eur Polym J* 1988, 24, 1029.
  26. Storey, R. F.; Taylor, A. E. *Polym Prepr* 1994, 35, 822.